
Low-Complexity Data-Parallel Earth Mover’s Distance Approximations

Kubilay Atasu¹ Thomas Mittelholzer²

Abstract

The Earth Mover’s Distance (EMD) is a state-of-the-art metric for comparing probability distributions. The high distinguishability offered by the EMD comes at a high cost in computational complexity. Therefore, linear-complexity approximation algorithms have been proposed to improve its scalability. However, these algorithms are either limited to vector spaces with only a few dimensions or require the probability distributions to populate the vector space sparsely. We propose novel approximation algorithms that overcome both of these limitations, yet still achieve linear time complexity. All our algorithms are data parallel, and therefore, we can take advantage of massively parallel computing engines, such as Graphics Processing Units (GPUs). The experiments on MNIST images show that the new algorithms can perform a billion distance computations in less than a minute using a single GPU. On the popular text-based 20 News-groups dataset, the new algorithms are four orders of magnitude faster than the state-of-the-art FastEMD library and match its search accuracy.

1. Introduction

Earth Movers Distance (EMD) was initially proposed in the image retrieval field to quantify the similarity between images (Rubner et al., 1998). In the optimization theory, a more general formulation of EMD, called Wasserstein distance, has been used extensively to measure the distance between probability distributions (Villani, 2003). In statistics, an equivalent measure is known as Mallows distance (Levina & Bickel, 2001). This work uses the EMD measure for similiary search in image and text databases.

In the text retrieval domain, an adaptation of EMD, called Word Movers Distance (WMD), has emerged as a state-of-the-art semantic similarity metric (Kusner et al., 2015).

¹IBM Research - Zurich ²HSR Hochschule für Technik, Rapperswil. Correspondence to: Kubilay Atasu <kat@zurich.ibm.com>.

WMD captures semantic similarity by using the concept of word embeddings in the computation of EMD. Word embeddings map words into a high-dimensional vector space such that the words that are semantically similar are close to each other. These vectors can be pre-trained in an unsupervised way, e.g., by running Google’s Word2vec algorithm (Mikolov et al., 2013) on publicly available data sets. The net effect is that, given two sentences that cover the same topic, but have no words in common, traditional methods, such as cosine similarity, fail to detect the similarity. However, WMD detects and quantifies the similarity by taking the proximity between different words into account.

Wasserstein distance has important applications ranging from image and text retrieval to recovery of features from noisy astrophysical images using Generative Adversarial Networks (GANs). What makes Wasserstein-based approaches, such as EMD, attractive is their high search and classification accuracy. However, such an accuracy does not come for free. In general, the time complexity of computing these measures grows cubically in the size of the input probability distributions. Such a high complexity renders their use impractical for large datasets. Thus, there is a growing need for low-complexity approximation methods.

A linear complexity approximation algorithm for computing EMD in low-dimensional vector spaces was proposed (Shirdhonkar & Jacobs, 2008). The algorithm has linear complexity in the size of the inputs. However its complexity grows exponentially with the dimensionality of the underlying vector space. In practice, the method becomes intractable if the dimensionality of the vector space is larger than three. For instance, it is not applicable to WMD because the dimensionality of the embedding vectors is in the order of several hundreds when using WMD.

A linear-complexity algorithm for computing approximate EMD distances over high-dimensional vector spaces has also been proposed (Atasu et al., 2017). The algorithm, called Linear-Complexity Relaxed Word Mover’s Distance (LC-RWMD), achieves four orders of magnitude improvement in speed with respect to WMD. In addition, on compact and curated text documents, it computes high-quality search results that are comparable to those found by WMD.

Despite its scalability, the limitations of LC-RWMD are not well understood. Our analysis shows that 1) it is not appli-

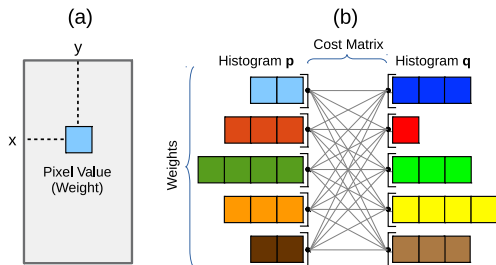


Figure 1. (a) Constructing a histogram from a greyscale image, b) Computing the EMD between two histograms.

cable to dense histograms, and 2) its accuracy decreases when comparing probability distributions with many overlapping coordinates. Our main contributions are as follows:

- We propose new distance measures that are more robust and provably more accurate than LC-RWMD.
- We show that the new measures effectively quantify the similarity between dense as well as overlapping probability distributions, e.g., greyscale images.
- We show that the new measures can be computed in linear time complexity in the size of the input probability distributions: the same as for LC-RWMD.
- We describe data-parallel implementations of the proposed distance computation algorithms and demonstrate their accuracy and runtime advantages on GPUs.

2. Background

EMD can be considered as the discrete version of the Wasserstein distance, and can be used to quantify the affinity between discrete probability distributions. Each probability distribution is modelled as a histogram, wherein each bin is associated with a weight and a coordinate in a multi-dimensional vector space. For instance, when measuring the distance between greyscale images, the histogram weights are given by the pixel values and the coordinates are defined by the respective pixel positions (see Fig. 1 (a)).

The distance between two histograms is calculated as the cost of transforming one into the other. Transforming a first histogram into a second one involves moving weights from the bins of the first histogram into the bins of the second, thereby constructing the second histogram from the first. The goal is to minimize the total distance travelled, wherein the pairwise distances between different histogram bins are computed based on their respective coordinates. This optimization problem is well studied in transportation theory and is the discrete formulation of the Wasserstein distance.

Assume that histograms \mathbf{p} and \mathbf{q} are being compared, where \mathbf{p} has h_p entries and \mathbf{q} has h_q entries. Assume also

that an $h_p \times h_q$ nonnegative cost matrix \mathbf{C} is available. Note that p_i indicates the weight stored in the i th bin of histogram \mathbf{p} , q_j indicates the weight stored in the j th bin of histogram \mathbf{q} , and $C_{i,j}$ indicates the distance between the coordinates of the i th bin of \mathbf{p} and the j th bin of \mathbf{q} (see Fig. 1 (b)). Suppose that the histograms are L^1 -normalized: $\sum_i p_i = \sum_j q_j = 1$.

We would like to discover a non-negative flow matrix \mathbf{F} , where $F_{i,j}$ indicates how much of the bin i of \mathbf{p} has to flow to the bin j of \mathbf{q} , such that the cost of moving \mathbf{p} into \mathbf{q} is minimized. Formally, the objective of EMD is as follows:

$$\text{EMD}(\mathbf{p}, \mathbf{q}) = \min_{F_{i,j} \geq 0} \sum_{i,j} F_{i,j} \cdot C_{i,j}. \quad (1)$$

A valid solution to EMD has to satisfy the so-called *out-flow* (2) and *in-flow* (3) constraints. The *out-flow* constraints ensure that, for each i of \mathbf{p} , the sum of all the flows exiting i is equal to p_i . The *in-flow* constraints ensure that, for each j of \mathbf{q} , the sum of all the flows entering j is equal to q_j . These constraints guarantee that all the mass stored in \mathbf{p} is transferred and \mathbf{q} is reconstructed as a result.

$$\sum_j F_{i,j} = p_i \quad (2)$$

$$\sum_i F_{i,j} = q_j \quad (3)$$

Computation of EMD requires solution of a minimum-cost-flow problem on a bi-partite graph, wherein the bins of histogram \mathbf{p} are the source nodes, the bins of histogram \mathbf{q} are the sink nodes, and the edges between the source and sink nodes indicate the pairwise transportation costs. Solving this problem optimally takes cubical time complexity in the size of the input histograms (Ahuja et al., 1993).

We would like to stress that in the framework of this work, which considers the discrete and not the continuous case of Wasserstein distances, the only requirement on the cost matrix is that it is nonnegative. Since any nonnegative cost c between two locations can be written as the p -th power of the p -th root of c for $p \geq 1$, one can assume that we are dealing with a p -th Wasserstein metric (Villani, 2008).

2.1. Relaxed Word Mover’s Distance

To reduce the complexity, an approximation algorithm called Relaxed Word Mover’s Distance (RWMD) was proposed (Kusner et al., 2015). RWMD computation involves derivation of two asymmetric distances. First, the *in-flow* constraints are relaxed and the relaxed optimization problem is solved using only *out-flow* constraints. The solution to the first relaxed problem is a lower bound on EMD. After that, the *out-flow* constraints are relaxed and a second relaxed optimization problem is solved using only *in-flow* constraints,

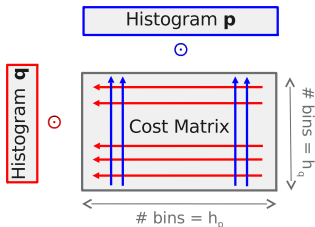


Figure 2. Quadratic-complexity RWMD computation

which computes a second a lower bound on EMD. RWMD is the maximum of these two lower bounds. Therefore, it is at least as tight as each one. In addition, it is symmetric.

Finding an optimal solution to RWMD involves mapping the coordinates of one histogram to the closest coordinates of the other. Just like EMD, RWMD requires a cost matrix C that stores the pairwise distances between coordinates of p and q . Finding the closest coordinates corresponds to row-wise and column-wise minimum operations in the cost matrix (see Fig. 2). To compute the first lower bound, it is sufficient to find the column-wise minimums in the cost matrix, and then perform a dot product with the weights stored in p . Similarly, to compute the second lower bound, it is sufficient to find the row-wise minimums and then perform a dot product with the weights stored in q . The complexity of RWMD is given by the cost of constructing the cost matrix C : it requires quadratic time and space in the size of the input histograms. Computing the row-wise and column-wise minimums of C also has quadratic time complexity.

2.2. Linear-Complexity RWMD

When computing RWMD between only two histograms, it is not possible to avoid a quadratic time complexity. However, in a typical information retrieval system, a query histogram is compared with a large database of histograms to identify the top-K most similar histograms in the database. It is shown in (Atasu et al., 2017) that in such cases, the RWMD computation involves redundant and repetitive operations, and eliminating the redundancy reduces the average time complexity from quadratic to linear.

Assume that a query histogram is being compared with two database histograms. Assume also that the two database histograms have common coordinates. A simple replication of the RWMD computation would involve creation of two cost matrices with identical rows for the common coordinates. Afterwards, it would be necessary to perform reduction operations on these identical rows to compute the row-wise minimums. It is shown in (Atasu et al., 2017) that both of these redundant operations can be eliminated by 1) constructing a vocabulary that stores the union of the coordinates that occur in the database histograms, and 2) computing the minimum distances between the coordinates of the vocabulary and the coordinates of the query only once.

Table 1. Algorithmic Parameters

n	Number of database histograms
v	Size of the vocabulary
m	Dimensionality of the vectors
h	Average histogram size

Table 2. Complexity Comparison

	Time Complexity	Space Complexity
LC-RWMD	$O(vhm + nh)$	$O(nh + vm + vh)$
RWMD	$O(nh^2m)$	$O(nhm)$

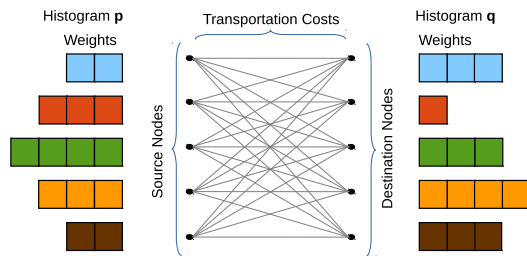


Figure 3. Different histograms with identical coordinates

Table 1 lists the algorithmic parameters that influence the complexity. Table 2 shows the complexity of RWMD and LC-RWMD algorithms when comparing one query histogram with n database histograms. When the number of database histograms (n) is in the order of the size of the vocabulary (v), the LC-RWMD algorithm reduces the complexity by a factor of the average histogram size (h). Therefore, whereas the time complexity of a brute-force RWMD implementation scales quadratically in the histogram size, the time complexity of LC-RWMD scales only linearly.

3. New Relaxation Algorithms

In this section, we describe improved relaxation algorithms that address the weaknesses of the RWMD measure and its linear-complexity implementation (LC-RWMD). Assume that we are measuring the distance between two histograms p and q . Assume also that the coordinates of the two histograms fully overlap but the respective weights are different (see Fig. 3). In other words, for each coordinate i of p , there is an identical coordinate j of q , for which $C_{i,j} = 0$. Therefore, RWMD estimates the total cost of moving p into q and vice versa as zero even though p and q are not the same. This condition arises, for instance, when we are dealing with dense histograms. In other cases, the data of interest might actually be sparse, but some background noise might also be present, which results in denser histograms.

In general, the more overlaps there are between the coordinates of p and q , the higher the approximation error of RWMD is. The main reason for the error is that when coordinate i of p overlaps with coordinate j of q , RWMD does

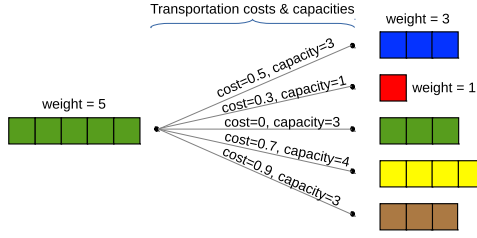


Figure 4. Imposing capacity constraints on the edges

not take into account the fact that the respective weights p_i and q_j can be different. In an optimal solution, we would not be moving a mass larger than the minimum of p_i and q_j between these two coordinates. This is a fundamental insight that we use in our improved solutions.

Given \mathbf{p} , \mathbf{q} and \mathbf{C} , our goal is to define new distance measures that relax fewer EMD constraints than RWMD, and therefore, produce tighter lower bounds on EMD. Two asymmetric distances can be computed by deriving 1) the cost of moving \mathbf{p} into \mathbf{q} and 2) the cost of moving \mathbf{q} into \mathbf{p} . If both are lower bounds on $\text{EMD}(\mathbf{p}, \mathbf{q})$, a symmetric lower bound can be derived, e.g., by using the maximum of the two. Thus, we consider only the computation of the cost of moving \mathbf{p} into \mathbf{q} without loss of essential generality.

When computing the cost of moving \mathbf{p} to \mathbf{q} using RWMD, the *in-flow* constraints of (3) are removed. In other words, all the mass is transferred from \mathbf{p} to the coordinates of \mathbf{q} , but the resulting distribution is not the same as \mathbf{q} . Therefore, the cost of transforming \mathbf{p} to \mathbf{q} is underestimated by RWMD. To achieve better approximations of $\text{EMD}(\mathbf{p}, \mathbf{q})$, instead of removing the *in-flow* constraints completely, we propose the use of a relaxed version of these constraints:

$$F_{i,j} \leq q_j \quad \text{for all } i, j. \quad (4)$$

The new constraint ensures that the amount of weight that can be moved from a coordinate i of \mathbf{p} to a coordinate j of \mathbf{q} cannot exceed the weight q_j at coordinate j . However, even if (4) is satisfied, the total weight moved to coordinate j of \mathbf{q} from all the coordinates of \mathbf{p} can exceed q_j , potentially violating (3). Namely, (3) implies (4), but not vice versa.

When (4) is used in combination with (2), we have:

$$F_{i,j} \leq \min(p_i, q_j) \quad \text{for all } i, j. \quad (5)$$

Note that we are essentially imposing capacity constraints on the edges of the flow network (see Fig.4) based on (5).

In the following subsections, we describe three new approximation methods. The Overlapping Mass Reduction (OMR) method imposes the relaxed constraint (4) only between overlapping coordinates, and is the lowest-complexity and the least accurate approximation method. The Iterative Constrained Transfers (ICT) method imposes

constraint (4) between all coordinates of \mathbf{p} and \mathbf{q} , and is the most complex and most accurate approximation method. The Approximate Iterative Constrained Transfers (AICT) method imposes constraint (4) incrementally between coordinates of \mathbf{p} and \mathbf{q} , and is an approximation of the ICT method. Therefore, both its complexity and its accuracy are higher than those of OMR, but lower than those of ICT.

3.1. Overlapping Mass Reduction

The OMR method imposes (4) only between overlapping coordinates. The main intuition behind OMR method is that if the coordinate i of \mathbf{p} and the coordinate j of \mathbf{q} overlap (i.e., $C_{i,j} = 0$), a transfer of $\min(p_i, q_j)$ can take place free of cost between \mathbf{p} of \mathbf{q} . After that, the remaining weight in p_i is transferred simply to the second closest coordinate in \mathbf{q} as this is the next least costly move. Therefore, the method computes only the top-2 smallest values in each row of \mathbf{C} . A detailed description is given in Algorithm 1.

Algorithm 1 Optimal Computation of OMR

```

1: function OMR( $\mathbf{p}, \mathbf{q}, \mathbf{C}$ )
2:    $t = 0$   $\triangleright$  initialize transportation cost  $t$ 
3:   for  $i = 1 \dots, h_p$  do  $\triangleright$  iterate the indices of  $\mathbf{p}$ 
4:      $s = \text{argmin}_2(C_{i, [1 \dots h_q]})$   $\triangleright$  find top-2 smallest
5:     if  $C_{i, s[1]} == 0$  then  $\triangleright$  if the smallest value is 0
6:        $r = \min(p_i, q_{s[1]})$   $\triangleright$  size of max. transfer
7:        $p_i = p_i - r$   $\triangleright$  move  $r$  units of  $p_i$  to  $q_{s[1]}$ 
8:        $t = t + p_i \cdot C_{i, s[2]}$   $\triangleright$  move the rest to  $q_{s[2]}$ 
9:     else
10:       $t = t + p_i \cdot C_{i, s[1]}$   $\triangleright$  move all of  $p_i$  to  $q_{s[1]}$ 
11:    end if
12:  end for
13:  return  $t$   $\triangleright$  return transportation cost  $t$ 
14: end function
    
```

3.2. Iterative Constrained Transfers

The ICT method imposes the constraint (4) between all coordinates of \mathbf{p} and \mathbf{q} . The main intuition behind the ICT method is that because the inflow constraint (3) is relaxed, the optimal flow exiting each source node can be determined independently. For each source node, finding the optimal flow involves sorting the destination nodes in the ascending order of transportation costs, and then performing iterative mass transfers between the source node and the sorted destination nodes under the capacity constraints (4). Algorithm 2 describes the ICT method in full detail.

Algorithm 3 describes an approximate solution to ICT (AICT), which offers the possibility to terminate the ICT iterations before all the mass is transferred from \mathbf{p} to \mathbf{q} . After performing a predefined number $k - 1$ of ICT iterations, the mass remaining in \mathbf{p} is transferred to the k -th closest coordinates of \mathbf{q} , making the solution approximate.

Algorithm 2 Optimal Computation of ICT

```

1: function ICT( $\mathbf{p}, \mathbf{q}, \mathbf{C}$ )
2:    $t = 0$   $\triangleright$  initialize transportation cost  $t$ 
3:   for  $i = 1 \dots, h_p$  do  $\triangleright$  iterate the indices of  $\mathbf{p}$ 
4:      $\mathbf{s} = \text{argsort}(C_{i,[1\dots h_q]})$   $\triangleright$  sort indices by value
5:      $l = 1$   $\triangleright$  initialize  $l$ 
6:     while  $p_i > 0$  do  $\triangleright$  while there is mass in  $p_i$ 
7:        $r = \min(p_i, q_{\mathbf{s}[l]})$   $\triangleright$  size of max. transfer
8:        $p_i = p_i - r$   $\triangleright$  move  $r$  units of  $p_i$  to  $q_{\mathbf{s}[l]}$ 
9:        $t = t + r \cdot C_{i,\mathbf{s}[l]}$   $\triangleright$  update cost
10:       $l = l + 1$   $\triangleright$  increment  $l$ 
11:    end while
12:  end for
13:  return  $t$   $\triangleright$  return transportation cost  $t$ 
14: end function
    
```

Theorem 1 establishes the optimality of Algorithm 2. Theorem 2 establishes the relationship between different distance measures. The proofs are given in Appendix A. The complexity of the algorithms are derived in Appendix B.

Theorem 1. (i) The flow F^* of Algorithm 2 is an optimal solution of the relaxed minimization problem given by (1), (2) and (4). (ii) ICT provides a lower bound on EMD.

Theorem 2. For two normalized histograms \mathbf{p} and \mathbf{q} : $RWMD(\mathbf{p}, \mathbf{q}) \leq OMR(\mathbf{p}, \mathbf{q}) \leq AICT(\mathbf{p}, \mathbf{q}) \leq ICT(\mathbf{p}, \mathbf{q}) \leq EMD(\mathbf{p}, \mathbf{q})$.

Algorithm 3 Approximate Computation of ICT

```

1: function AICT( $\mathbf{p}, \mathbf{q}, \mathbf{C}, k$ )
2:    $t = 0$   $\triangleright$  initialize transportation cost  $t$ 
3:   for  $i = 1 \dots, h_p$  do  $\triangleright$  iterate the indices of  $\mathbf{p}$ 
4:      $\mathbf{s} = \text{argmin}_k(C_{i,[1\dots h_q]})$   $\triangleright$  find top- $k$  smallest
5:      $l = 1$   $\triangleright$  initialize  $l$ 
6:     while  $l < k$  do
7:        $r = \min(p_i, q_{\mathbf{s}[l]})$   $\triangleright$  size of max. transfer
8:        $p_i = p_i - r$   $\triangleright$  move  $r$  units of  $p_i$  to  $q_{\mathbf{s}[l]}$ 
9:        $t = t + r \cdot C_{i,\mathbf{s}[l]}$   $\triangleright$  update cost
10:       $l = l + 1$   $\triangleright$  increment  $l$ 
11:    end while
12:    if  $p_i \neq 0$  then  $\triangleright$  if  $p_i$  still has some mass
13:       $t = t + p_i \cdot C_{i,\mathbf{s}[k]}$   $\triangleright$  move the rest to  $q_{\mathbf{s}[k]}$ 
14:    end if
15:  end for
16:  return  $t$   $\triangleright$  return transportation cost  $t$ 
17: end function
    
```

4. Linear-Complexity Implementations

In this section, we focus on the AICT method because 1) it is a generalization of all the other methods presented, and 2) its complexity and accuracy can be controlled by setting the number k of iterations performed. We describe a

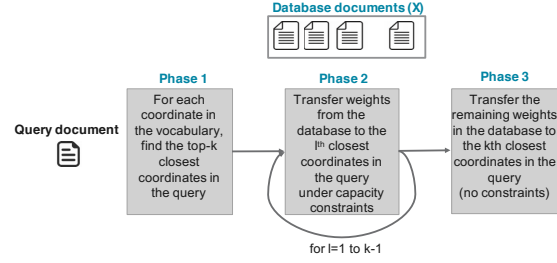


Figure 5. Linear Complexity AICT

linear complexity implementation of AICT and derive its complexity bounds. Unlike the previous section, we do not assume that the cost matrix is given, but we compute the transportation costs on the fly. Our analysis takes into account the complexity of computing these costs as well.

A high-level view of the linear-complexity AICT algorithm (LC-AICT) is given in Figure 5. LC-AICT is strongly inspired by LC-RWMD. Just like LC-RWMD, it assumes that 1) a query histogram is compared with a large number of database histograms, and 2) the coordinate space is populated by the members of a fixed-size vocabulary. Like LC-RWMD, LC-AICT eliminates the redundant and repetitive operations when comparing one query histogram with a large number of database histograms.

Suppose that the dimension of the coordinates is m and the size of the vocabulary is v . Let \mathbf{V} be an $v \times m$ matrix that stores this information. Given a query histogram \mathbf{q} of size h , we construct a matrix \mathbf{Q} of size $h \times m$ that stores the coordinates of the histogram entries. Phase 1 of LC-AICT (see Fig. 6) performs a matrix-matrix multiplication between \mathbf{V} and the transpose of \mathbf{Q} to compute all pairwise distances between the coordinates of the vocabulary and the coordinates of the query. The result is a $v \times h$ distance matrix, denoted by \mathbf{D} . As a next step, the top- k smallest distances are computed in each row of \mathbf{D} . The result is stored in a $v \times k$ matrix \mathbf{Z} . Furthermore, we store the indices of \mathbf{q} that are associated with the top- k smallest distances in a $v \times k$ matrix \mathbf{S} . We can then construct another $v \times k$ matrix \mathbf{W} , which stores the corresponding weights of \mathbf{q} by defining $\mathbf{W}_{i,l} = \mathbf{q}_{\mathbf{S}_{i,l}}$ for $i = 1, \dots, v$ and $l = 1, \dots, k$. The matrices \mathbf{Z} and \mathbf{W} are then used in Phase 2 to transport the largest possible mass, which are constrained by \mathbf{W} , to the smallest possible distances, which are given by \mathbf{Z} .

The database histograms are stored in a matrix \mathbf{X} (see Fig. 7), wherein each row stores one histogram. These histograms are typically sparse. Thus, the matrix \mathbf{X} is stored using a sparse representation, e.g., in compressed sparse rows (csr) format. For simplicity, assume that \mathbf{X} is stored in a dense format and $\mathbf{X}_{u,i}$ stores the weight of the i -th coordinate of the vocabulary in the u -th database histogram. If the histograms have h entries on average, the number of nonzeros in matrix \mathbf{X} would be equal to nh .

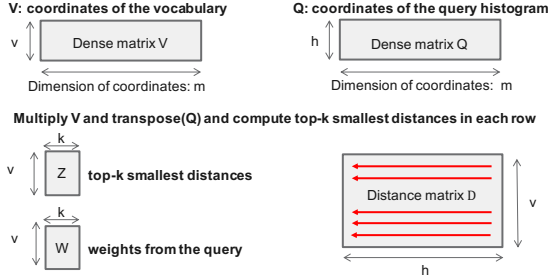


Figure 6. Phase 1 of LC-AICT

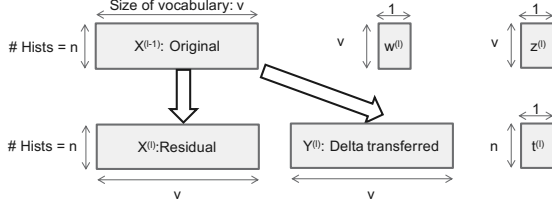


Figure 7. Phase 2 of LC-AICT

Phase 2 of AICT iterates the columns of \mathbf{Z} and \mathbf{W} and iteratively transfers weights from the database histograms \mathbf{X} to the query histogram q . Let $\mathbf{X}^{(l)}$ represent the residual mass remaining in \mathbf{X} after l iterations, where $\mathbf{X}^{(0)} = \mathbf{X}$. Let $\mathbf{Y}^{(l)}$ store the amount of mass that is transferred from $\mathbf{X}^{(l-1)}$ in iteration l , which is the difference between $\mathbf{X}^{(l-1)}$ and $\mathbf{X}^{(l)}$. Let $\mathbf{z}^{(l)}$ and $\mathbf{w}^{(l)}$ be the l -th columns of \mathbf{Z} and \mathbf{W} , respectively; thus, $z_u^{(l)}$ is the l -th smallest distance between the coordinate u of the vocabulary and the coordinates of the query, and $w_u^{(l)}$ is the respective weight of the query coordinate that produces the l -th smallest distance. The iteration l of Phase 2 computes $\mathbf{Y}^{(l)}$ and $\mathbf{X}^{(l)}$:

$$\mathbf{Y}_{u,i}^{(l)} = \min_{\substack{u \in \{1 \dots v\} \\ i \in \{1 \dots v\}}} (\mathbf{X}_{u,i}^{(l-1)}, w_u^{(l)}). \quad (6)$$

$$\mathbf{X}^{(l)} = \mathbf{X}^{(l-1)} - \mathbf{Y}^{(l)}. \quad (7)$$

The cost of transporting $\mathbf{Y}^{(l)}$ to q is given by $\mathbf{Y}^{(l)} \cdot \mathbf{z}^{(l)}$. Let $\mathbf{t}^{(l)}$ be a vector of size n that accumulates all the transportation costs incurred between iteration 1 and iteration l :

$$\mathbf{t}^{(l)} = \mathbf{t}^{(l-1)} + \mathbf{Y}^{(l)} \cdot \mathbf{z}^{(l)}. \quad (8)$$

After $k - 1$ iterations of Phase 2, there might still be some mass remaining in $\mathbf{X}^{(k-1)}$. Phase 3 approximates the cost of transporting the remaining mass to q by multiplying $\mathbf{X}^{(k-1)}$ with $\mathbf{z}^{(k)}$. The overall transportation cost $\mathbf{t}^{(k)}$ is:

$$\mathbf{t}^{(k)} = \mathbf{t}^{(k-1)} + \mathbf{X}^{(k-1)} \cdot \mathbf{z}^{(k)}. \quad (9)$$

The main building blocks of the LC-AICT algorithm are matrix-matrix or matrix-vector multiplications, row-wise top- k calculations, and parallel element-wise updates. All of these operations are data-parallel and can be vectorized on GPUs. Table 3 shows the time and space complexity of LC-AICT. Appendix B provides the respective derivations.

 Table 3. Complexity of LC-AICT (k iterations)

Time	Space
$O(vhm + knh)$	$O(nh + vm + vh + vk)$

5. Experiments

We performed experiments on two public datasets: *20 Newsgroups*¹ is a text database of approximately 20k newsgroup documents, partitioned evenly across 20 different classes, and *MNIST* is an image database² of 60k greyscale hand-written digits that are partitioned evenly across 10 classes that represent digits. The MNIST images are mapped to two-dimensional histograms as illustrated in Fig. 1, wherein the weights are normalized pixel values. The words in 20 Newsgroups documents are mapped to a high-dimensional embedding space using Google's word and phrase vectors that are pre-trained on Google News³, for which the size of the vocabulary (v) is 3M words and phrases, and embedding vectors are composed of $m = 300$ single-precision floating-point numbers. In case of the 20 Newsgroups dataset, the histogram weights are determined by normalizing the frequencies of the words and phrases.

We treated each document of the database as a query and compared it with every other document in the database. Based on the distance measure used in the comparison, for each query document, we identified the top- K nearest neighbors in the database. After that, for each query document, we computed the percentage of documents in its nearest-neighbors list that have the same label. We averaged this metric over all the database documents and computed it as a function of K . The result is the average *precision @ top- K* for the whole database, which indicates the expected accuracy of nearest neighbors search queries.

We compared our distance measures with cosine similarity and the Word Centroid Distance (WCD) measures, both of which exhibit a low algorithmic complexity. Note that the cosine similarity method does not use the proximity information provided by the embedding vectors. The complexity of computing cosine similarity between one query histogram and n database histograms is $O(nh)$. The WCD measure (Kusner et al., 2015) computes a centroid vector of size m for each document, which is a weighted average of the embedding vectors. Given the centroids, the complexity of computing WCD between one query document and n database documents is $O(nm)$. Note that the complexity of the methods we propose are in the order of $O(nhm)$, i.e., higher than both. The reason is that we take into account all the words that occur in the documents individually as well as their proximity to each other.

¹<http://qwone.com/~jason/20Newsgroups/>

²<http://yann.lecun.com/exdb/mnist/>

³<https://code.google.com/archive/p/word2vec/>

Table 4. Runtime (seconds)

	WCD	Cosine	RWMD	OMR	AICT (1)
20 News	4.2	7.3	39.6	57.1	59.3
MNIST	12.7	30.7	35.1	152.5	200.7

We developed data-parallel and GPU-accelerated implementations of the WCD, RWMD, OMR, AICT, and cosine similarity methods and evaluated their performance on an NVIDIA® GTX 1080Ti GPU (see Tab. 4). The runtime overhead of the proposed methods is less than 50% with respect to RWMD for 20 Newsgroups. In addition, despite the relatively large number of dimensions ($m = 300$), the runtime increase w.r.t. cosine similarity is less than ten fold. In case of MNIST, because the number of dimensions is small ($m = 2$), RWMD is as fast as the cosine similarity. However, the runtime of the Phase 2 of the AICT method is more significant than that of its Phase 1. The runtime increase w.r.t. cosine similarity is still less than ten fold. Notably, in case of the MNIST database, 3.6 billion AICT computations were performed in about 3.3 minutes only.

Figure 8 compares different distance measures using the 20 Newsgroups dataset. The OMR measure consistently outperforms cosine similarity, RWMD, and WCD measures. A single iteration of AICT measure improves the precision further. Additional iterations of AICT contribute a marginal improvement in the precision, and are not shown. Note that the improvement achieved over cosine similarity and RWMD increases as a function of K. We also observe that there is no essential difference between the precision of AICT and of the state-of-the-art FastEMD library⁴.

The FastEMD library solves an approximation of EMD by applying a thresholding technique (Pele & Werman, 2009). The approximation preserves the metric properties of EMD and reduces the runtime by an order of magnitude. In our experiments, we simply used the default threshold values of FastEMD. To speed-it up further, we applied the RWMD-based pruning technique described in the WMD paper (Kusner et al., 2015). In addition, we developed a multi-threaded implementation of the pruning technique, and deployed it on an 8-core Intel® i7-6900K CPU. These optimisations resulted in an approximately two-orders-of-magnitude reduction of the runtime of FastEMD. Despite all our optimisations, obtaining FastEMD results on the complete 20 Newsgroups dataset took three weeks. On the other hand, OMR and AICT methods performed the same number of distance computations in less than a minute. Therefore, we are reporting a 30000-fold performance improvement with respect to a highly-optimized FastEMD implementation without any essential loss of accuracy (see Tab. 5). These results show that the OMR and the AICT

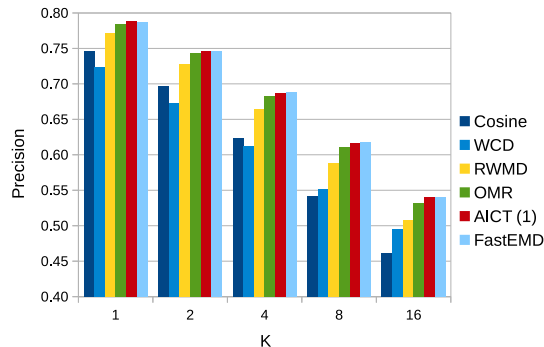


Figure 8. Precision @ top-K for 20 Newsgroups

Table 5. AICT vs FastEMD for 20 Newsgroups

	AICT (1)	FastEMD
Precision @ top-16	0.5409	0.5408
Runtime (minutes)	< 1	30033

measures are meaningful on their own, and using more complex distance measures, such as FastEMD does not necessarily improve the accuracy of nearest-neighbors search.

Note that a GPU-implementation of the FastEMD algorithm is not readily available. It is not a GPU-friendly algorithm either as it does not rely on data-parallel operations. On the other hand, all our algorithms are data-parallel, and map well to GPUs. Our GPU implementations typically result in a ten- to twenty-fold improvement of the performance with respect to the respective CPU implementations.

Figure 9 compares different distance measures using the MNIST dataset. In this case, the number of dimensions is too small for WCD to be effective. However, the images are normalized and centered, which makes the cosine similarity extremely effective. Nevertheless, the methods we propose consistently outperform cosine similarity. Even though the improvements are modest in comparison to 20 Newsgroups results, the differences become more evident for large K. In this case, computing FastEMD results on the full MNIST dataset is not feasible computationally. However, our experiments on a small subset of MNIST confirm what we observe for 20 Newsgroups: FastEMD does not offer any essential accuracy improvement with respect to AICT.

Theorem 2 states that the more complex the considered algorithms, the smaller the gap to the EMD and, hence, the better the accuracy. The least complex AICT algorithm is the RWMD, which corresponds to the AICT (0) with zero iterations in Phase 2 (see Fig. 5). The second most complex algorithm is the OMR. In Fig. 8, the most complex AICT algorithm is AICT (1) with a single iteration in Phase 2. In Fig. 9, the most complex AICT algorithm is AICT (10) with ten iterations in Phase 2. In these figures, the search accuracy improves with the complexity and, thus, illustrates the accuracy vs complexity trade-off. Typically, most of

⁴<https://github.com/LeeKamentsky/pyemd>

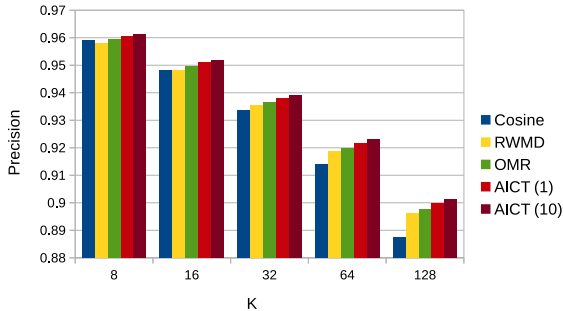


Figure 9. Precision @ top-K for MNIST (without background)

Table 6. Precision @ top-K for MNIST (with background)

K	WCD	Cosine	RWMD	OMR	AICT (10)
1	0.2644	0.9770	0.1123	0.9707	0.9771
16	0.1398	0.9479	0.1002	0.9368	0.9504
128	0.1061	0.8873	0.1002	0.8692	0.8977

the improvement in the search accuracy is achieved by the first iteration of Phase 2, and subsequent iterations result in a limited improvement only. As a result, AICT (1) offers very favorable accuracy and runtime combinations.

Table 6 illustrates the sensitivity of RWMD to a minor change in the data representation. Here, we simply explore the impact of including the background (i.e. the black pixels) in the MNIST histograms. The most immediate result is that when comparing two histograms, all their coordinates overlap. As a result, the distance computed between the histograms by RWMD is always equal to zero, and the top-K nearest neighbors are randomly selected, resulting in a precision of 10% for RWMD. The OMR technique solves this problem immediately even though its accuracy is lower than that of cosine similarity. In fact, several iterations of AICT are required to outperform the cosine similarity results. However, these results prove the improved robustness and effectiveness of our methods in comparison to RWMD.

6. Related Work

There is a growing interest in applying optimal transport theory to emerging machine learning problems (Cuturi & Solomon, 2017). It has been shown that Wasserstein distance can be used as the loss function when training GANs and auto-encoders, and doing so improves the stability of the training algorithms (Arjovsky et al., 2017; Gulrajani et al., 2017) as well as the quality of the samples that are generated (Tolstikhin et al., 2018).

A regularized version of the optimal transport problem can be solved more efficiently than the traditional network-flow-based approaches, but leads to approximate results (Cuturi, 2013). The solution algorithm is based on Sinkhorn’s matrix scaling technique (Sinkhorn, 1964),

and thus, it is called Sinkhorn’s algorithm. The algorithm may require up to $O(h)$ iterations for convergence, and the complexity of each iteration is $O(h^2)$. Therefore, its worst-case time complexity is $O(h^3)$. Sinkhorn’s algorithm converges much faster than network-flow-based approaches (Solomon et al., 2015). In addition, a greedy coordinate-descent-based solution method can reduce the complexity of the Sinkhorn’s algorithm to $O(h^2 \log h)$ (Altschuler et al., 2017). However, methods that rely on Sinkhorn’s algorithm exhibit a significantly higher worst-case time complexity than our methods. In addition, Sinkhorn-based methods do not compute lower or upper bounds of EMD and suffer from numerical stability issues, requiring some parameter tuning to be effective.

Several other lower bounds of EMD have been proposed (Assent et al., 2008; Xu et al., 2010; Ruttenberg & Singh, 2011; Wichterich et al., 2008; Xu et al., 2016; Huang et al., 2016; 2014). These lower bounds are typically used to speed-up the EMD computation based on pruning techniques. Alternatively, EMD can be computed approximately using a compressed representation (Uysal et al., 2016; Pele & Werman, 2009). A greedy approximation algorithm related to ours was proposed (Gottschlich & Schuhmacher, 2014), but it does not relax the *in-flow* or *out-flow* constraints. Therefore, it is not data-parallel and its complexity is quadratic in the histogram size. In addition, it produces an upper bound rather than a lower bound of EMD. We are not aware of other approximations that both achieve a linear time complexity and offer a search accuracy as high as ours.

7. Conclusions

This paper provides novel theoretical and practical results for improving the efficiency and scalability of approximate EMD computation over high-dimensional histograms. We identify the main shortcomings of the RWMD measure and propose new related distance measures that result in an improved search accuracy and robustness without increasing the computational complexity. Under realistic assumptions, the complexity of our methods scale linearly in the size of the histograms. In high dimensions, our methods result in an only 50% increase in the runtime in comparison to a linear-complexity implementation of RWMD. We also propose data-parallel implementations that are suitable for GPU acceleration, and demonstrate a 30000-fold performance improvement with respect to a multi-threaded implementation of WMD without sacrificing any accuracy. Our experiments prove the effectiveness of our methods on both sparse text-based and dense image-based datasets. Future work includes comparing our methods with regularized optimal transport techniques in terms of speed and accuracy.

8. Acknowledgements

We would like to thank Celestine Dünner and Haralampos Pozidis from IBM Research for their technical comments.

References

- Ahuja, R. K., Magnanti, T. L., and Orlin, J. B. *Network Flows: Theory, Algorithms, and Applications*. Prentice-Hall, Inc., Upper Saddle River, NJ, USA, 1993. ISBN 0-13-617549-X.
- Altschuler, J., Weed, J., and Rigollet, P. Near-linear time approximation algorithms for optimal transport via sinkhorn iteration. In Guyon, I., Luxburg, U. V., Bengio, S., Wallach, H., Fergus, R., Vishwanathan, S., and Garnett, R. (eds.), *Advances in Neural Information Processing Systems 30*, pp. 1964–1974. Curran Associates, Inc., 2017.
- Arjovsky, M., Chintala, S., and Bottou, L. Wasserstein generative adversarial networks. In Precup, D. and Teh, Y. W. (eds.), *Proceedings of the 34th International Conference on Machine Learning*, volume 70 of *Proceedings of Machine Learning Research*, pp. 214–223, International Convention Centre, Sydney, Australia, 06–11 Aug 2017. PMLR.
- Assent, I., Wichterich, M., Meisen, T., and Seidl, T. Efficient similarity search using the Earth Mover's Distance for large multimedia databases. In *2008 IEEE 24th International Conference on Data Engineering (ICDE)*, pp. 307–316, April 2008.
- Atasu, K., Parnell, T. P., Dünner, C., Sifalakis, M., Pozidis, H., Vasileiadis, V., Vlachos, M., Berrospi, C., and Labbi, A. Linear-complexity relaxed word mover's distance with GPU acceleration. In *2017 IEEE International Conference on Big Data, BigData 2017, Boston, MA, USA, December 11-14, 2017*, pp. 889–896, 2017.
- Cuturi, M. Sinkhorn distances: Lightspeed computation of optimal transport. In Burges, C. J. C., Bottou, L., Welling, M., Ghahramani, Z., and Weinberger, K. Q. (eds.), *Advances in Neural Information Processing Systems 26*, pp. 2292–2300. Curran Associates, Inc., 2013.
- Cuturi, M. and Solomon, J. M. A primer on optimal transport. Tutorial at *Advances in Neural Information Processing Systems (NIPS) 30*, 12 2017.
- Gottschlich, C. and Schuhmacher, D. The shortlist method for fast computation of the earth mover's distance and finding optimal solutions to transportation problems. *PLOS ONE*, 9(10):1–10, 10 2014.
- Gulrajani, I., Ahmed, F., Arjovsky, M., Dumoulin, V., and Courville, A. C. Improved training of Wasserstein GANs. In Guyon, I., Luxburg, U. V., Bengio, S., Wallach, H., Fergus, R., Vishwanathan, S., and Garnett, R. (eds.), *Advances in Neural Information Processing Systems 30*, pp. 5767–5777. Curran Associates, Inc., 2017.
- Huang, J., Zhang, R., Buyya, R., and Chen, J. MELODY-JOIN: Efficient Earth Mover's Distance similarity joins using MapReduce. In *2014 IEEE 30th International Conference on Data Engineering (ICDE)*, pp. 808–819, March 2014.
- Huang, J., Zhang, R., Buyya, R., Chen, J., and Wu, Y. Heads-Join: Efficient Earth Mover's Distance Similarity Joins on Hadoop. *IEEE Transactions on Parallel and Distributed Systems*, 27(6):1660–1673, 2016.
- Kusner, M., Sun, Y., Kolkin, N., and Weinberger, K. From word embeddings to document distances. In Bach, F. and Blei, D. (eds.), *Proceedings of the 32nd International Conference on Machine Learning*, volume 37 of *Proceedings of Machine Learning Research*, pp. 957–966, Lille, France, 07–09 Jul 2015. PMLR.
- Levina, E. and Bickel, P. The Earth Mover's distance is the Mallows distance: some insights from statistics. In *Proceedings Eighth IEEE International Conference on Computer Vision. ICCV 2001*, volume 2, pp. 251–256, 2001. ISBN 0-7695-1143-0. doi: 10.1109/ICCV.2001.937632.
- Mikolov, T., Chen, K., Corrado, G., and Dean, J. Efficient estimation of word representations in vector space. *CoRR*, abs/1301.3781, 2013.
- Pele, O. and Werman, M. Fast and robust earth mover's distances. In *2009 IEEE 12th International Conference on Computer Vision*, pp. 460–467, Sept 2009.
- Rubner, Y., Tomasi, C., and Guibas, L. J. A metric for distributions with applications to image databases. In *Proceedings of the Sixth International Conference on Computer Vision, ICCV '98*, pp. 59–66, Washington, DC, USA, 1998. IEEE Computer Society. ISBN 81-7319-221-9.
- Ruttenberg, B. E. and Singh, A. K. Indexing the earth mover's distance using normal distributions. *Proceedings of the VLDB Endowment*, 5(3):205–216, 2011.
- Shirdhonkar, S. and Jacobs, D. W. Approximate earth movers distance in linear time. In *2008 IEEE Conference on Computer Vision and Pattern Recognition*, pp. 1–8, June 2008.
- Sinkhorn, R. A Relationship Between Arbitrary Positive Matrices and Doubly Stochastic Matrices. *The Annals of Mathematical Statistics*, 35(2):876–879, 1964.

- Solomon, J., de Goes, F., Peyré, G., Cuturi, M., Butscher, A., Nguyen, A., Du, T., and Guibas, L. Convolutional wasserstein distances: Efficient optimal transportation on geometric domains. *ACM Trans. Graph.*, 34(4):66:1–66:11, July 2015. ISSN 0730-0301.
- Tolstikhin, I., Bousquet, O., Gelly, S., and Schoelkopf, B. Wasserstein auto-encoders. In *International Conference on Learning Representations*, 2018.
- Uysal, M. S., Sabinasz, D., and Seidl, T. Approximation-based efficient query processing with the Earth Mover's Distance. In *Proceedings, Part II, of the 21st International Conference on Database Systems for Advanced Applications - Volume 9643*, DASFAA 2016, pp. 165–180, New York, NY, USA, 2016. Springer-Verlag New York, Inc. ISBN 978-3-319-32048-9.
- Villani, C. *Topics in Optimal Transportation*, volume 58 of *Graduate Studies in Mathematics*. AMS, 2003 edition, 2003. ISBN 978-0-8218-3312-4.
- Villani, C. *Optimal Transport: Old and New*. Grundlehren der mathematischen Wissenschaften. Springer, 2009 edition, September 2008. ISBN 3540710493.
- Wichterich, M., Assent, I., Kranen, P., and Seidl, T. Efficient EMD-based similarity search in multimedia databases via flexible dimensionality reduction. In *Proceedings of the 2008 ACM SIGMOD International Conference on Management of Data*, SIGMOD '08, pp. 199–212, New York, NY, USA, 2008. ACM. ISBN 978-1-60558-102-6.
- Xu, J., Zhang, Z., Tung, A. K., and Yu, G. Efficient and effective similarity search over probabilistic data based on earth mover's distance. *Proceedings of the VLDB Endowment*, 3(1-2):758–769, 2010.
- Xu, J., Zhang, J., Song, C., Zhang, Q., Lv, P., Li, T., and Chen, N. EMD-DSJoin: Efficient similarity join over probabilistic data streams based on Earth Mover's Distance. In *Web Technologies and Applications*, pp. 42–54. Springer International Publishing, 2016.

A. Optimality and Effectiveness

Alg. 2 computes an optimum flow \mathbf{F}^* , whose components are determined by the quantities r in step 4. Namely, the components of the i -th row of \mathbf{F}^* , are given recursively as $F_{i,s[1]}^* = \min(p_i, q_{s[1]})$ and $F_{i,s[l]}^* = \min(p_i - \sum_{u=1}^{l-1} F_{i,s[u]}^*, q_{s[l]})$ for $l = 2, \dots, h_q$.

Lemma 1. *Each row i of the flow \mathbf{F}^* of Algorithm 2 has a certain number k_i , $1 \leq k_i \leq h_q$ of nonzero components, which are given by $F_{i,s[l]}^* = q_{s[l]}$ for $l = 1, \dots, k_i - 1$ and $F_{i,s[k_i]}^* = p_i - \sum_{l=1}^{k_i-1} q_{s[l]}$.*

The Lemma follows by keeping track of the values of the term r in step 4 in Alg. 2. An immediate implication is that the flow F^* satisfies the constraints (2) and (4). One can also show that F^* is a minimal solution of (1) under the constraints (2) and (4), and this leads to the following theorem.

Theorem 1. (i) *The flow F^* of Algorithm 2 is an optimal solution of the relaxed minimization problem given by (1), (2) and (4).* (ii) *ICT provides a lower bound on EMD.*

Proof. Proof of part (i): It has already been shown that the flow \mathbf{F}^* satisfies constraints (2) and (4), and it remains to show that \mathbf{F}^* achieves the minimum in (1). To this end, let \mathbf{F} be any nonnegative flow, which satisfies (2) and (4). To show that \mathbf{F}^* achieves the minimum in (4), it is enough to show that for every row i , one has $\sum_j F_{i,j} C_{i,j} \geq \sum_j F_{i,j}^* C_{i,j}$, which then implies $\sum_{i,j} F_{i,j} C_{i,j} \geq \sum_{i,j} F_{i,j}^* C_{i,j}$.

By Alg. 2, there is a reordering given by the list \mathbf{s} such that

$$C_{i,s[1]} \leq C_{i,s[2]} \leq \dots \leq C_{i,s[n_q]}. \quad (10)$$

By Lemma 1, there is a $k_i \leq n_q$ such that $\sum_{l=1}^{k_i} F_{i,s[l]}^* = p_i$ and $F_{i,s[l]}^* = 0$ for $l > k_i$. Furthermore by Lemma 1 and by constraint (4) on \mathbf{F} , it follows that

$$F_{i,s[l]} \leq q_{s[l]} = F_{i,s[l]}^* \quad \text{for } l = 1, \dots, k_i - 1. \quad (11)$$

The outflow-constraint (2) implies $\sum_j F_{i,j} = p_i = \sum_j F_{i,j}^*$ or, equivalently,

$$\sum_{l=k_i}^{n_q} F_{i,s[l]} = F_{i,s[k_i]}^* + \sum_{l=1}^{k_i-1} (F_{i,s[l]}^* - F_{i,s[l]}). \quad (12)$$

In the following chain of inequalities, the first inequality follows from (10), and (12) implies the equality in the second step.

$$\begin{aligned} \sum_{l=k_i}^{n_q} C_{i,s[l]} F_{i,s[l]} &\geq C_{i,s[k_i]} \sum_{l=k_i}^{n_q} F_{i,s[l]} \\ &= C_{i,s[k_i]} (F_{i,s[k_i]}^* + \sum_{l=1}^{k_i-1} (F_{i,s[l]}^* - F_{i,s[l]})) \\ &= C_{i,s[k_i]} F_{i,s[k_i]}^* + \sum_{l=1}^{k_i-1} C_{i,s[k_i]} (F_{i,s[l]}^* - F_{i,s[l]}) \\ &\geq C_{i,s[k_i]} F_{i,s[k_i]}^* + \sum_{l=1}^{k_i-1} C_{i,s[l]} (F_{i,s[l]}^* - F_{i,s[l]}). \end{aligned}$$

The inequality in the last step follows from (10) and the fact that the terms $F_{i,s[l]}^* - F_{i,s[l]}$ are nonnegative by (11). By

rewriting the last inequality, one obtains the desired inequality

$$\begin{aligned} \sum_j F_{i,j} C_{i,j} &= \sum_{l=1}^{n_q} F_{i,s[l]} C_{i,s[l]} \\ &\geq \sum_{l=1}^{k_i} F_{i,s[l]}^* C_{i,s[l]} \\ &= \sum_j F_{i,j}^* C_{i,j}, \end{aligned}$$

where in the last equation $F_{i,s[l]}^* = 0$ for $l > k_i$ is used.

Proof of part (ii): Since ICT is a relaxation of the constrained minimization problem of the EMD, ICT provides a lower bound on EMD given by the output of Alg. 2, namely, $\sum_{i,j} F_{i,j}^* C_{i,j} = \text{ICT}(\mathbf{p}, \mathbf{q}) \leq \text{EMD}(\mathbf{p}, \mathbf{q})$. □

Similar to Alg. 2, Alg. 3 also determines an optimum flow F^* , which now depends on the number of iterations k .

Lemma 2. *Each row i of the flow \mathbf{F}^* of Algorithm 3 has a certain number k_i , $1 \leq k_i \leq k$ of nonzero components, which are given by $F_{i,s[l]}^* = q_{s[l]}$ for $l = 1, \dots, k_i - 1$ and $F_{i,s[k_i]}^* = p_i - \sum_{l=1}^{k_i-1} q_{s[l]}$.*

Based on this Lemma, one can show that the flow F^* from Algorithm 3 is an optimum solution to the minimization problem given by (1), (2) and (4), in which the constraint (4) is further relaxed in function of the predetermined parameter k . Since the constrained minimization problems for ICT, AICT, OMR, RWMD form a chain of increased relaxations of EMD, one obtains the following result.

Theorem 2. *For two normalized histograms \mathbf{p} and \mathbf{q} : $\text{RWMD}(\mathbf{p}, \mathbf{q}) \leq \text{OMR}(\mathbf{p}, \mathbf{q}) \leq \text{AICT}(\mathbf{p}, \mathbf{q}) \leq \text{ICT}(\mathbf{p}, \mathbf{q}) \leq \text{EMD}(\mathbf{p}, \mathbf{q})$.*

We call a nonnegative cost function \mathbf{C} *effective*, if for any indices i, j , the equality $C_{i,j} = 0$ implies $i = j$. For a topological space, this condition is related to the Hausdorff property. For an effective cost function \mathbf{C} , one has $C_{i,j} > 0$ for all $i \neq j$, and, in this case, $\text{OMR}(\mathbf{p}, \mathbf{q}) = \sum_{i,j} C_{i,j} F_{i,j}^* = 0$ implies $F_{i,j}^* = 0$ for $i \neq j$ and, thus, $k_i = 1$ in Lemma 2 and, thus, \mathbf{F}^* is diagonal with $F_{i,i}^* = p_i$. This implies $p_i \leq q_i$ for all i and, since both histograms are normalized, one must have $\mathbf{p} = \mathbf{q}$.

Theorem 3. *If the cost function \mathbf{C} is effective, then $\text{OMR}(\mathbf{p}, \mathbf{q}) = 0$ implies $\mathbf{p} = \mathbf{q}$, i.e., OMR is effective.*

Remark 1. *If OMR is effective, then, a fortiori, AICT and ICT are also effective. However, RWMD does not share this property.*

B. Complexity Analysis

The algorithms presented in Section 3 assume that the cost matrix \mathbf{C} is given, yet they still have a quadratic time complexity in the size of the histograms. Assume that the histograms size is h . Then, the size of \mathbf{C} is h^2 . The complexity is determined by the row-wise reduction operations on \mathbf{C} . In case of the OMR method, the top-2 smallest values are computed in each row of \mathbf{C} and a maximum of two updates are performed on each bin of \mathbf{p} . Therefore, the complexity is $O(h^2)$. In case of the AICT method, the top- k smallest values are computed in each row, and up to k updates are performed on each histogram bin. Therefore, the complexity is $O(h^2 \log k + hk)$. The ICT method is the most expensive one because 1) it fully sorts the rows of \mathbf{C} , and 2) it requires $O(h)$ iterations in the worst case. Its complexity is given by $O(h^2 \log h)$.

In Section 4, the complexity of Phase 1 of the LC-AICT algorithm is $O(vhm + nh \log k)$ because the complexity of the matrix multiplication that computes \mathbf{D} is $O(vhm)$, and the complexity of computing top- k smallest distances in each row of \mathbf{D} is $O(nh \log k)$. The complexity of performing (6), (7), (8), and (9) are $O(nh)$ each. When $k - 1$ iterations of Phase 2 is applied, the overall time complexity of the LC-AICT algorithm is $O(vhm + knh)$. Note that when the number of iterations k performed by LC-AICT is a constant, LC-AICT and LC-RWMD have the same time complexity. When the number of iterations are in the order of the dimensionality of the coordinates (i.e., $O(k) = O(m)$) and the database is sufficiently large (i.e., $O(n) = O(v)$), LC-AICT and LC-RWMD again have the same time complexity, which increases linearly in the size of the histograms h . In addition, the sizes of the matrices \mathbf{X} , \mathbf{V} , \mathbf{D} , and \mathbf{Z} are nh , vm , vh , and vk , respectively. Therefore, the overall space complexity of the LC-AICT algorithm is $O(nh + vm + vh + vk)$.